NASA Technical Memorandum 83655
AIAA-84-1161

Performance of a High-Work Low Aspect Ratio Turbine Tested with a Realistic Inlet Radial Temperature Profile

Roy G. Stabe, Warren J. Whitney,
and Thomas P. Moffitt
Lewis Research Center
Cleveland, Ohio

Prepared for the
Twentieth Joint Propulsion Conference
cosponsored by the AIAA, SAE, and ASME
Cincinnati, Ohio, June 11-13, 1984

NASA

PERFORMANCE OF A HIGH-WORK LOW ASPECT RATIO TURBINE TESTED WITH A REALISTIC INLET RADIAL TEMPERATURE PROFILE

Roy G. Stabe, Warren J. Whitney, and Thomas P. Moffitt
National Aeronautics and Space Administration
Lewis Research Center
Cleveland, Ohio 44135

Abstract

Experimental results are presented for a 0.767 scale model of the first stage of a two-stage turbine designed for a high by-pass ratio engine. The turbine was tested with both uniform inlet conditions and with an inlet radial temperature profile simulating engine conditions. The inlet temperature pr. ile was essentially mixed-out in the rotor. There was also substantial underturning of the exit flow at the mean diameter. Both of these effects were attributed to strong secondary flows in the rotor blading. There were no significant differences in the stage performance with either inlet condition when differences in tip clearance were considered. Performance was very close to design intent in both cases.

Nomenclature

b	vane or blade height, cm
c_x	chord axial length, cm
D	diameter, cm
$\bar{e}$	kinetic energy loss coefficient, $\frac{V^2/U_{2d}^2}{1 - V^2/V_{1d}^2}$
Δh	specific work, J/kg
N	rotative speed, rpm
p	pressure, N/m^2 abs
s	spacing, cm
T	absolute temperature, K
U	blade velocity, m/sec
V	absolute gas velocity, m/sec
W	relative gas velocity, m/sec
w	mass flow, kg/sec
x	axial dimensional, cm
α	absolute gas flow angle measured from axial direction, deg
β	relative gas flow angle measured from axial direction, deg
γ	ratio of specific heats
δ	ratio of inlet total pressure to U.S. standard sea-level pressure, p_0/p^*
ϵ	function of γ used in relating parameters to those using air inlet conditions at U.S. standard sea-level conditions, $(0.73959/\gamma)[(\gamma+1)/2]^{\gamma/(\gamma-1)}$
η	total efficiency (based on inlet-total to exit-total) pressure ratio
θ_{cr}	squared ratio of critical velocity at turbine inlet to critical velocity at U.S. standard sea-level air $(V_{cr}/V_{cr}^*)^2$

Subscripts

cr	condition corresponding to Mach number of unity
id	ideal process
m	mean section
0	station at CERTS inlet
x	axial direction
1	station at turbine inlet
2	station at stator exit
3	station at turbine exit

Superscripts

'	absolute total state
"	relative total state
*	U.S. standard sea-level conditions (temperature equal to 288.15 K pressure equal to $10.132 N/m^2$ abs x 10^4 psia)
----	average value

Summary

Experimental results are presented for a 0.767 scale model of the first stage of a two-stage turbine designed for a high by-pass ratio engine. The turbine was tested with both uniform inlet conditions and with an inlet radial temperature profile simulating engine conditions. The inlet temperature profile was essentially mixed-out in the rotor. There was also substantial underturning of the exit flow at the mean diameter. Both of these effects were attributed to strong secondary flows in the rotor blading. There were no significant differences in the stage performance with either inlet condition when differences in tip clearance were considered. Performance was very close to design intent in both cases.

Introduction

The modern high bypass ratio aircraft engine, in comparison to earlier engines, requires a higher specific work, lower equivalent flow high pressure turbine due to higher engine pressure ratios. If this turbine were designed with conventional stator angles of about 65°, the result would be a turbine with transonic Mach numbers, very short blades, and, consequently, poor performance. Very flat stator angles, 75° or more from axial, alleviate these problems. But turbine performance correlation in common use such as Stewart,[1] or Smith,[2] indicate that there is a substantial penalty for using such large stator angles due to increased turning and secondary flow losses. However, by carefully designing the blading for good surface velocity distributions using computational techniques such as Refs. 3 and 4, much of the penalty due to high turning might be avoided. The efficiency could then be maintained at essentially the same level as a more conventional turbine designed for a low bypass ratio engine.

An investigation of the characteristics of turbine blading for use in high bypass ratio engines is in progress at the NASA Lewis Research Center. A series of stator vanes designed for good surface velocity distribution and with exit angles ranging from 67 to 80° was tested in a two-dimensional cascade. The results, reported in Ref. 5, show a modest increase in the energy loss coefficient from 0.02 for the 67° vane to 0.025 for the 80° vane. This small increase in loss would affect the efficiency of a two-stage turbine with a 75° stator by only about 0.1 percent. This paper presents the test results of the first stage

of a two-stage high pressure turbine suitable for use in a high bypass ratio engine.

The test turbine was a 0.767 scale model of the engine size turbine, it was tested in the NASA Lewis Research Center's Warm Core Turbine Test Facility.[6] This facility includes an inlet section which generates inlet radial temperature and pressure profiles similar to those found in flight engines. The turbine was tested with inlet temperature and pressure profile at design speed and pressure ratio. The principal objective of these tests was to determine how much the highly loaded, low aspect ratio blading of this turbine would attenuate the inlet temperature profile. Performance testing was done over a range of speeds and pressure ratios with uniform inlet conditions. In both cases, at design speed and pressure ratio, radial surveys of inlet total pressure and temperature and also of exit total pressure, temperature and flow angle were made 2-1/2 chords downstream of the rotor. Additional surveys of exit total temperature were made at locations 3/4 and 1-1/2 chords downstream of the rotor. Some of these results were compared to an analytical procedure in Ref. 7. This paper presents a description of the turbine design, turbine performance in terms of mass flow, specific work and efficiency and compares the results of the exit radial surveys with uniform inlet conditions and with an inlet radial temperature profile.

Apparatus and Procedure

Turbine Design

The test turbine was to be the first stage of a two stage high pressure turbine suitable for use in a high bypass ratio engine. The design point conditions used in the design were similar to those of the Energy Efficient Engine Program. These are listed in Table I. A parametric study was done to aid in determining the overall turbine geometry. The criteria used in this study were: subsonic blading, reasonable blade height, and rotor turning limited to about 110° at the mean section. A turbine with a 60.96 cm (24 in.) mean diameter and a 75° stator exit angle best met these criteria. This was then scaled down to a mean diameter of 46.736 cm to better match the warm core turbine test facility. The balance of this discussion pertains to the 0.767 scale model turbine.

The turbine velocity diagrams are shown in Fig. 1. The stator and rotor geometry are listed in Tables II and III, respectively. The stator vane is a constant section, constant angle design and both stator and rotor endwalls are cylindrical to simplify manufacture. The rotor inlet was designed to accept the stator exit flow with zero or slight negative incidence as calculated by Ref. 3. The rotor outlet is a free-vortex design. Both vane and blade axial chords are constant radially. The dimensions of the axial chords and also of the leading and trailing edge radii were kept similar to an earlier, more conventional and more lightly loaded core turbine for which considerable test data is available.[8-10] This was done to keep the aspect ratios and leading and trailing edge geometry of the two turbines similar. The efficiency of the reference turbine, 0.89 adjusted to 1 percent tip clearance, was also used as the design point of the subject turbine in the absence of recent published data on the performance of highly loaded, high-turning vanes and blades. The objective was to design the blading with surface velocity distributions which would maintain this efficiency. A second objective was a low number of blades. This further increases loading but it decreases cooling air requirement and cost. The final design had 26 vanes and 48 blades.

The methods of Refs. 3 and 4 were used to calculate the surface velocities. A trial profile was laid out and the velocities calculated. The profile was changed as necessary and the process repeated until a satisfactory surface velocity distribution was obtained. The final vane and blade surface velocities for the hub, mean and tip sections are shown in Figs. 2(a) and (b), respectively. The vane and blade coordinates are listed in Tables IV and V.

The blade sections were stacked to form a ruled surface to simplify machining. The stacking axis is a radial line through the section centroids. This procedure compromised the surface velocity distribution at the hub section where there is a diffusion on the pressure surface near the leading edge which would cause a separation bubble at this location. A modification of these blades is in progress which will eliminate this problem. The vanes were stacked on a radial line at 71.4 percent of the axial chord. This results in a larger stream sheet thickness in the throat region of the hub section and reduces the suction surface velocities at this location. Photographs of the stator and rotor installed in the test rig are shown in Figs. 3(a) and (b), respectively.

Test Facility

A photograph of the turbine test facility, which has been described in some detail in Ref. 6, is shown in Fig. 4. The turbine inlet air was supplied from the laboratory 40 psig combustion air system. The pressure was controlled with a 10 in. manually operated main valve and a 6 in. automatically controlled bypass valve. The air was heated with 3 can-type combustors using natural gas as fuel. The air flow was measured with a calibrated commercially available venturi meter. The fuel rate was measured with a flow nozzle. After passing through the turbine the air was throttled to the laboratory altitude exhaust system through a 24 in. butterfly valve.

The turbine power was absorbed with an eddy current dynamometer and dissipated, as heat to the cooling water, in the dynamometer stator. The turbine output torque was measured with a brushless rotating torque meter which was installed on the shaft between the turbine and dynamometer. A back-up torque measurement was also made on the dynamometer stator. The turbine rotative speed was measured with an electronic counter and a 60-tooth gear which was mounted on the turbine shaft.

The turbine inlet radial temperature profile was adjusted by individually controlling and metering the flow of coolant air through each of the four CERTS inlet section infusion slots shown in Fig. 5. CERTS is an acronym for "Combustor Exit Radial Temperature Simulator."

Test Rig Instrumentation

Test rig inlet (station "0") temperature upstream of the CERTS slots was measured with 20 thermocouples, five on each of the four inlet struts.

The average turbine inlet (station "1") temperature was calculated from measured flow rate and temperature values of primary and CERTS air flows. Static pressure was determined from five static taps each on the inner and outer wall. Also at this plane were two small shielded total temperature probes and one total pressure probe mounted in actuators for radial surveys of turbine inlet total pressure and temperature. The pressure probe's stem was electrically insulated from the turbine casing so that probe contact with the hub wall could be detected. The probe tip was a 0.5 mm tube flattened to 0.35 mm. The resultant temperature and pressure profiles taken at design point conditions are shown in Fig. 6. Both the temperature and pressure profiles contribute to an outlet radial velocity profile which affected analytically determined secondary flows[7].

Static pressure between the stator and rotor (station "2") was determined from 17 static taps each on the hub and tip walls. These taps were closely spaced across one vane exit passage.

The turbine exit (station "3", 2-1/2 blade chords downstream of blade exit) instrumentation consisted of six static taps each on the hub and tip walls and four combination probes. These probes were mounted in self-aligning actuators and were used for radial surveys of exit flow angle, total temperature, and total pressure.

Additional radial exit temperature surveys were taken at 3/4 and 1-1/2 blade chords downstream of the blade exit. Three touch probe clearance measuring devices were spaced around the outer casing over the rotor blade to measure clearance. Also, vane surface static pressure distributions were determined from 10 static taps each on the vane hub, mean, and tip location.

Procedure

The turbine was tested with and without the CERTS air turned on. Actual work output was determined from torque, speed, and mass flow rate measurements. Ideal work was based on inlet total temperature and calculated inlet and exit total pressures.

Turbine inlet temperature was calculated from a heat balance between the primary and CERTS flows. Turbine inlet and exit total pressures were both calculated from continuity based on measured static pressures, mass flow rate, flow angles, and total temperatures. The exit total temperature was calculated from calculated values of inlet total temperature and work output.

Results and Discussion

The results of this investigation are presented in two parts. The first covers the overall performance of the turbine stage operating with uniform inlet conditions. These include: mass flow, specific work, and efficiency data for a range of speeds and pressure ratios. The second covers the results of the exit radial surveys of temperature, pressure and flow angle at design speed and pressure ratio. The results for the stage operating with an inlet radial temperature profile are compared with the results obtained with uniform inlet conditions.

Overall Performance

The variation of equivalent mass flow with total-to-total pressure ratio and speed is shown in Fig. 7. The curve is drawn through the design speed data. There is a small speed effect on the flow indicating that the rotor controlled flow. The rotor was apparently choked at higher pressure ratios. At design pressure ratio, 2.36, the equivalent mass flow was 3.12 kg/sec, 0.6 percent higher than the design value.

Equivalent specific work for the range of total-to-total pressure ratios and speeds investigated is shown in Fig. 8. The turbine developed slightly more than design equivalent specific work, 56 300 J/Kg, at the design pressure ratio. There was very little difference in specific work between the 100 and 110 percent design equivalent speed lines except at the highest pressure ratios. The flattening of the curves for speeds less than 110 percent indicated a limiting loading condition occurred at a total-to-total pressure ratio of about 3.5.

The stage total efficiency for the same range of speed and pressure ratio as for specific work is shown in Fig. 9. The indicated efficiency at design speed and pressure ratio is 0.895 compared to the design value of 0.890. The peak efficiency is 0.902 at 110 percent design speed and a total-to-total pressure ratio of 2.6. There are no peak values for the lower speeds. The efficiency drops-off gradually at the lower pressure ratios and then more rapidly as the limiting load condition is approached.

Rotor Exit Radial Survey Results

The results of the radial surveys of rotor exit total temperature at three axial locations are shown in Fig. 10. The data shown at 3/4 and 1-1/2 chords axially downstream of the rotor were measured with a single actuated probe. At 2-1/2 chords the data is the average of measurements from four probes. The curves shown compare the exit temperatures with a uniform inlet temperature to the exit temperatures with an inlet radial temperature profile generated by the CERTS inlet (fig. 6(a)). The data shown is normalized by the average inlet temperature which was 672 K for both inlet conditions. Figure 10 shows that there is some mixing and flattening of the inlet temperature profile as the flow moves downstream. However, the inlet temperature profile is essentially mixed-out 3/4 chords axially downstream of the rotor. The analysis of Ref. 7 shows strong secondary flows in this blading. These secondary flows are the probable cause of the temperature mixing.

The results of radial surveys of exit flow angle and also the exit critical velocity ratio calculated from measured total pressure and wall static pressure are shown in Figs. 11(a) and (b), respectively. The data shown are the average measurements from four combination probes located about 2-1/2 chords downstream of the rotor exit. The

corresponding rotor relative exit flow angle and critical velocity ratio are shown in Figs. 12(a) and (b). Data are shown for three inlet conditions: Uniform - 422 K, Uniform - 672 K, and the radial temperature profile generated by the CERTS inlet section (fig. 6(a)) also with an average temperature of 672 K. The radial variation of exit absolute flow angle, shown in Fig. 11(a), deviated substantially from design intent. At the mean section the flow is underturned 13°. The flow angle variation for all three inlet conditions is about the same from the hub wall to the blade mean section. From the mid-section to the tip wall, however, the radial variation in flow angle depended strongly on rotor tip clearance. The average tip clearance for each inlet condition is noted on Fig. 11(a). The annulus area average flow angle for a uniform inlet temperature of 422 K, the condition at which the performance data was taken, was 23.2°, 7° less than design. The radial variations of exit critical velocity ratio shown in Fig. 11(b) are similar to each other for all three cases and seem less dependant on tip clearance. The exit velocity was higher than design at the mean section and lower at the hub wall. The combination of angle and velocity results show that there was a fairly large shift in mass flow from the hub to the mean section and that there was a larger than design loss at the hub wall. The average value of $(V/V_{cr})_3$, calculated from continuity using 23.2° as the average flow angle and wall static pressure measurements was 0.384 compared to 0.394 design. The preponderance of underturning at the mean section was probably caused by secondary flows in the rotor passage; the same mechanism responsible for mixing the radial temperature profile.

The radial variation of relative flow angle and exit velocity ratio, shown in Figs. 12(a) and (b), respectively, were calculated from the data shown in Fig. 11 and total temperature from the radial surveys. The radial variation in relative flow angle for the two uniform inlet conditions, which had the smallest tip clearance, were almost the same over the entire blade span. The effect of the larger tip clearance which occurred with CERTS inlet condition is still evident and results in about 3° more under turning over most of the blade span between the mean and tip sections. There is much less radial variation in the relative velocity ratio (fig. 12(b)), than there was for the absolute velocities. The relative velocity ratios roughly parallel the design radial variation but at a lower level. The average relative flow angle and critical velocity ratio, for a uniform inlet condition at 422 K were 66.5° and 0.841, respectively, compared to the design values of 67.8° and 0.867.

The efficiency of the turbine operating with either of the two uniform inlet conditions was 0.895. The rotor tip clearance ranged between 0.5 and 0.8 percent for these conditions. The efficiency when operating with a inlet temperature profile was a point less, 0.855 and the tip clearance was larger, 1.2 percent of blade height. The difference in efficiency can be attributed to the larger tip clearance. Aside from the effect of tip clearance the performance of this turbine was essentially the same with an inlet temperature profile or uniform inlet conditions.

A mean section velocity diagram representative of the stage performance was calculated from data and is compared to design diagram in Fig. 13. The stator exit velocity was higher than design resulting in about 5° positive incidence at the rotor inlet and also lower than design rotor reaction. The lower reaction accounts for the lower than design rotor exit velocities and also for the 7° average underturning discussed above as more work was done as a result of the higher rotor inlet targential momentum. The higher stator velocities are also evident in the vane surface velocities calculated from surface static pressure measurements. These are shown in Fig. 2(a). The surface velocities shown at the vane hub section are high enough that they might have caused substantially higher than design loss at this section. This would account for the higher than design loss observed at the rotor exit hub section (fig. 11(b)).

Stator and rotor loss determined from test data and from the turbine performance prediction method of Ref. 11 along with the design values are summarized in Table VI. The stator loss determined from data was 0.073, substantially higher than the design loss or the loss predicted by the reference method. The stator loss accounts for about 1.5 percent decrement in stage efficiency compared to the design loss. The rotor loss determined from data was 0.119 and agrees very well with the predicted loss. Both experimental and predicted loss are substantially lower than the design value and account for a two percent increase in stage efficiency compared to the design loss. The predicted efficiency, 0.907, appears attainable if the blading were modified to restore design rotor reaction and reduce the stator velocities particularly at the hub section.

Summary of Results

A 0.767 scale model of the first stage of a two stage high pressure turbine designed for a high bypass ratio engine was tested in the Warm Core Turbine Test Facility at NASA Lewis Research Center. The turbine was tested with both uniform inlet conditions and with an inlet radial temperature profile simulating engine conditions.

(1) The turbine met or slightly exceeded the design goals for efficiency, specific work and equivalent mass flow at design pressure ratio.

(2) There was significant underturning of the rotor exit flow particularly at the mean section. At design speed and pressure ratio the average exit flow angle was 23.2° compared to the 30.2° design angle. At the mean section the underturning was 13°. From the mean to the tip blade sections, this underturning was strongly dependent on tip clearance.

(3) The inlet radial temperature profile was essentially mixed out in the rotor. Radial surveys of rotor exit temperature at three axial locations showed little difference between exit temperatures when the turbine operated with uniform inlet conditions or with an inlet temperature profile.

(4) There were essentially no differences in the overall performance of this turbine with uniform inlet condition or with an inlet radial

temperature profile when differences in tip clearance were considered.

(5) Analytical studies available at this time indicate that strong secondary flows in the low-aspect ratio, high turning blading caused both the rotor exit flow underturning and the inlet radial temperature profile mixing observed in this turbine test.

References

1. Stewart, W. L., "A Study of Axial Flow Turbine Efficiency Characteristics in Terms of Velocity Diagram Parameters, ASME Paper-61-WA-37, Nov. 1961.

2. Smith, S. F., "A Simple Correlation of Turbine Efficiency, Journal of the Royal Aeronautical Society, Vol. 69, No. 655, July 1965, pp. 467-470.

3. Katsanis, T. and McNally, W. D., "Revised FORTRAN Program for Calculating Velocities and Streamlines on the Hub-Shroud Midchannel Stream Surface of an Axial-, Radial-, or Mixed-Flow Turbomachine or Annular Duct -- I User's Manual, NASA-TN-D-8430, 1977.

4. Katsanis, T., "FORTRAN Program for Calculating Transonic Velocities on a Blade-to-Blade Stream Surface of a Turbomachine, NASA-TN-D-5427, 1969.

5. Schwab, J. R., "Aerodynamic Performance of High Turning Core Turbine Vanes in a Two-Dimensional Cascade, NASA-TM-82894, 1982.

6. Whitney, W. J., Stabe, R. G., and Moffitt, T. P., "Description of the Warm Core Turbine Facility Recently Installed at NASA Lewis Research Center, NASA-TM-81562, 1980.

7. Schwab, J. R., Stabe, R. G., and Whitney, W T., "Analytical and Experimental Study of Flow Through an Axial Turbine Stage with a Nonuniform Inlet Radial Temperature Profile, NASA-TM-83431, 1983.

8. Szanca, E. M., Schum, H. J., and Hotz, G. M., "Research Turbine for High Temperature Core Engine Application - I Cold-Airoverall Performance of Solid Scaled Turbine, NASA-TN-D-7557, 1974.

9. Goldman, L. J. and McLallin, K. L., "Cold-Air Annular-Cascade Investigation of Aerodynamic Performance of Core-Engine-Cooled Turbine Vanes - I Solid-Vane Performance and Facility Description. NASA-TM-X-3224, 1975.

10. Stabe, R. G. and Kline, J. F., "Incidence Loss For a Core Turbine Rotor Blade in a Two-Dimensional Cascade. NASA-TM-X-3047, 1974.

11. Boyle, R. J., Haas, J. E., and Katsanis, T., "Comparison Between Measured Turbine Stage Performance and the Predicted Performance Using Quasi 3-D Flow and Boundary Layer Analyses", AIAA Paper 84-1299, 1984.

TABLE I. - TURBINE DESIGN AND TEST CONDITIONS

	Test			Standard air equivalent
	Design	Uniform inlet	Certs inlet	
Mean diameter, Dm, cm	60.96	46.744	46.744	46.744
Inlet total temperature, T_1', K	1533	422.2	672.2	288.2
Inlet total pressure, P_1' , $P_a x 10^{-4}$	124.1	31.03	31.03	10.13
Mass flow, W, Kg/sec	27.216	7.811	6.130	3.098
Specific work, Δh, J/Kgx10^{-4}	28.867	8.248	12.990	5.630
Rotative speed, N, rpm	13 000	9048	11 373	7475
Total pressure ratio, P_1'/P_3'	2.239	2.360	2.360	2.408
Work factor, $\Delta h/U_m^2$	1.675	1.675	1.675	1.675
Flow factor, V_x/U_m	0.449	0.449	0.449	0.449
Design efficiency	0.890	0.890	0.890	0.890

TABLE II. - TURBINE STATOR GEOMETRY

Mean diameter, D_m, cm	46.744
Mean vane pitch, s_m, cm	5.648
Vane height, b, cm	3.564
Axial chord, c_x, cm	3.556
Axial solidity, c_x/s_m	0.630
Aspect ratio, b/c_x	1.000
Number of vanes	26
Leading edge radius, cm	0.508
Trailing edge radius, cm	0.089
Zweifel coefficient	0.794

TABLE III. - TURBINE ROTOR GEOMETRY

Mean diameter, D_m, cm	46.744
Mean blade pitch, s_m, cm	3.059
Blade height, b, cm	3.564
Axial chord, c_x, cm	3.302
Axial solidity, c_x/s_m	1.079
Aspect ratio, b/c_x	1.077
Number of blades	48
Leading edge radius, cm	0.305
Trailing edge radius, cm	0.089
Zweifel coefficient	0.910

TABLE IV. - STATOR VANE COORDINATES

X	Y_L	Y_U	X	Y_L	Y_U
0.000	0.509	0.509	3.800	0.587	1.133
0.200	0.105	1.064	4.000	0.568	1.084
0.400	0.012	1.221	4.200	0.546	1.035
0.600	0.008	1.319	4.400	0.520	0.983
0.800	0.089	1.385	4.600	0.492	0.930
1.000	0.193	1.427	4.800	0.460	0.875
1.200	0.283	1.453	5.000	0.425	0.819
1.400	0.361	1.465	5.200	0.388	0.762
1.600	0.427	1.468	5.400	0.349	0.703
1.800	0.481	1.461	5.600	0.308	0.643
2.000	0.525	1.447	5.800	0.264	0.582
2.200	0.559	1.427	6.000	0.219	0.520
2.400	0.585	1.402	6.200	0.173	0.457
2.600	0.603	1.372	6.400	0.127	0.394
2.800	0.614	1.339	6.600	0.083	0.329
3.000	0.619	1.303	6.800	0.042	0.263
3.200	0.619	1.264	7.000	0.006	0.197
3.400	0.613	1.224	7.134	0.088	0.088
3.600	0.602	1.179			

TABLE V. - ROTOR BLADE COORDINATES

X	Hub		Mean		Tip	
	Orientation angle, ϕ_s deg					
	31.74		37.93		43.20	
	Y_L	Y_U	Y_L	Y_U	Y_L	Y_U
-0.011	0.521	0.521	-----	-----	-----	-----
- .004	-----	-----	0.441	0.441	-----	-----
0	0.280	0.762	.305	.580	0.305	0.305
0.200	.018	1.269	.018	1.139	.018	.955
.400	.015	1.472	.015	1.325	.015	1.162
.600	.215	1.582	.204	1.431	.192	1.272
.800	.501	1.640	.427	1.486	.373	1.332
1.000	.660	1.660	.559	1.506	.475	1.359
1.200	.750	1.646	.637	1.499	.537	1.362
1.400	.792	1.606	.676	1.471	.572	1.347
1.600	.798	1.544	.689	1.426	.589	1.319
1.800	.777	1.465	.681	1.368	.590	1.279
2.000	.739	1.373	.658	1.299	.579	1.230
2.200	.687	1.272	.624	1.222	.559	1.173
2.400	.625	1.162	.581	1.137	.531	1.109
2.600	.555	1.046	.531	1.047	.496	1.039
2.800	.478	.924	.476	.951	.457	.965
3.000	.396	.797	.415	.850	.414	.886
3.200	.308	.665	.350	.745	.366	.802
3.400	.215	.528	.281	.636	.316	.715
3.600	.119	.387	.209	.524	.262	.625
3.800	.018	.242	.134	.408	.206	.532
3.946	.089	.089	-----	-----	-----	-----
4.000	-----	-----	.056	.290	.148	.437
4.200	-----	-----	.009	.169	.088	.338
4.249	-----	-----	.089	.089	-----	-----
4.400	-----	-----	-----	-----	.026	.238
4.586	-----	-----	-----	-----	.089	.089

TABLE VI. - LOSS SUMMARY

		Experiment	Reference 11	Design
Stator	$\bar{e}$	0.073	0.046	0.05
	$\Delta\eta$	.043	.027	.026
	P_1'/P_2	1.704	1.704	1.568
Rotor	$\bar{e}$	0.119	0.116	0.153
	$\Delta\eta$	.062	.065	.084
	P_2''/P_3	1.652	1.650	1.685
Overall	η	0.895	0.907	0.890
	P_1'/P_3'	2.360	2.360	2.239

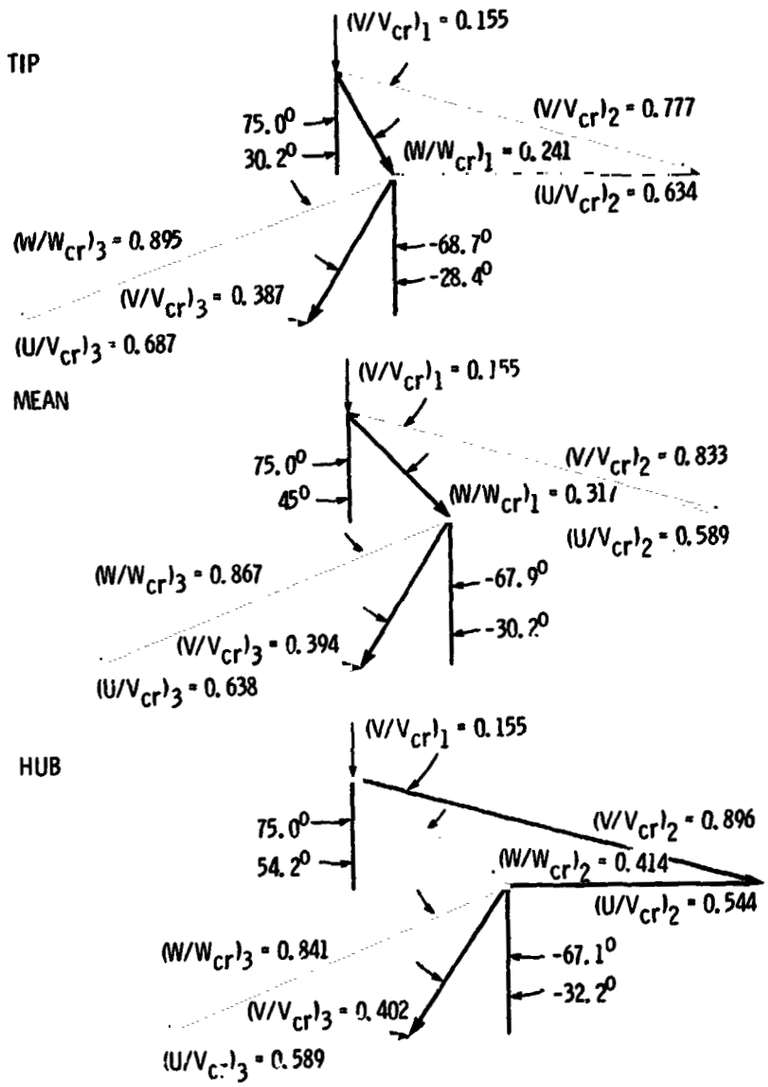

Figure 1. - Turbine design velocity diagrams.

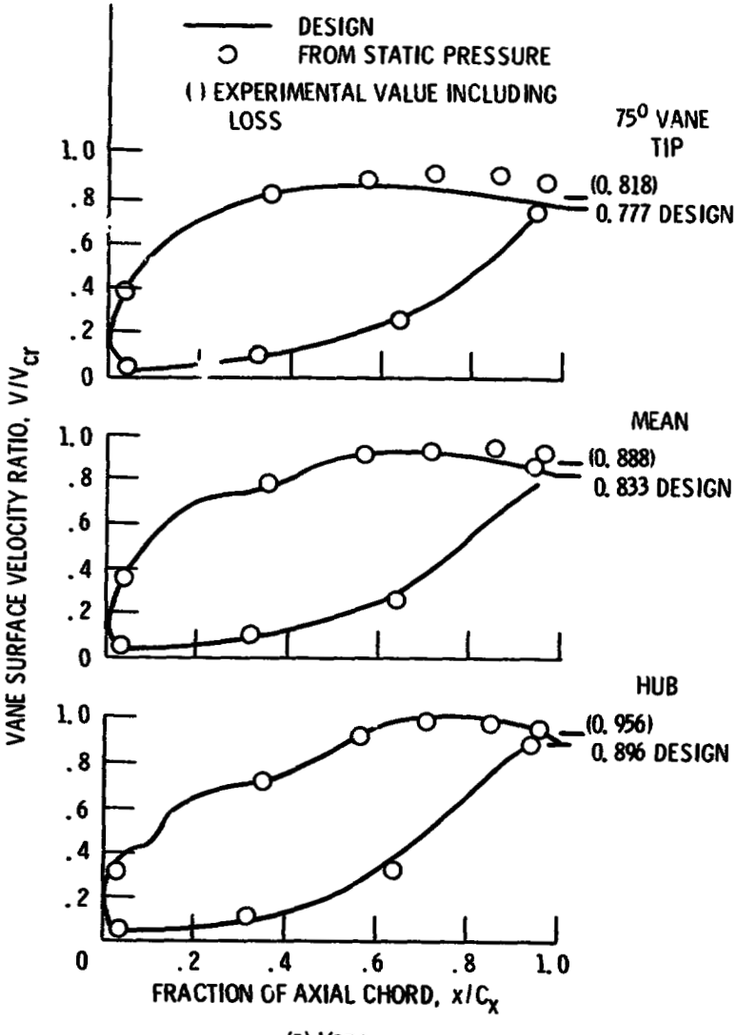

(a) Vane.

Figure 2. - Surface velocities.

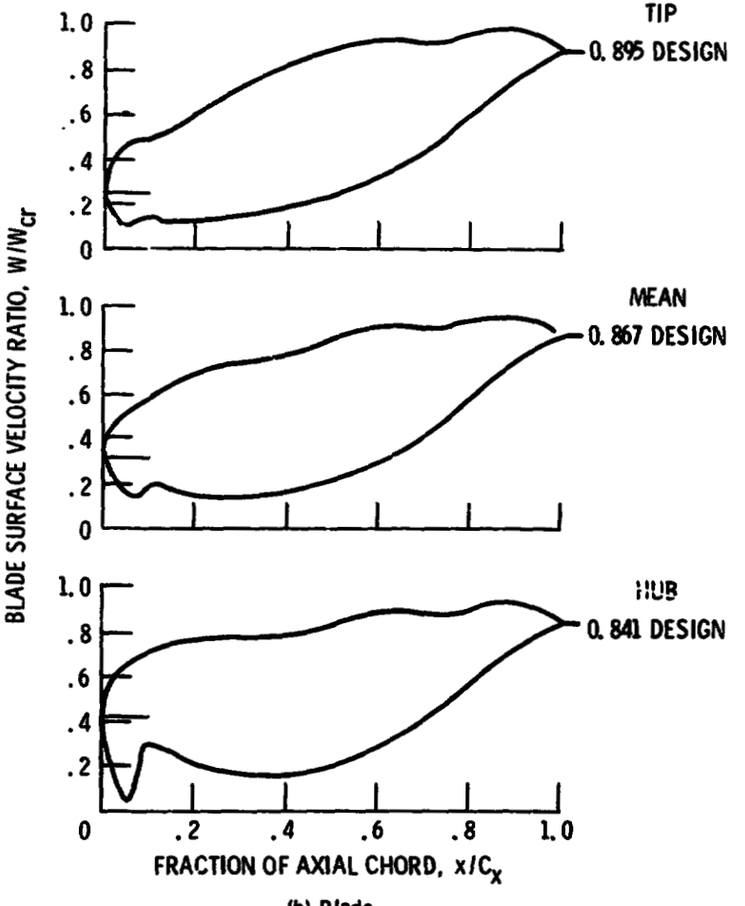

(b) Blade.

Figure 2. - Concluded.

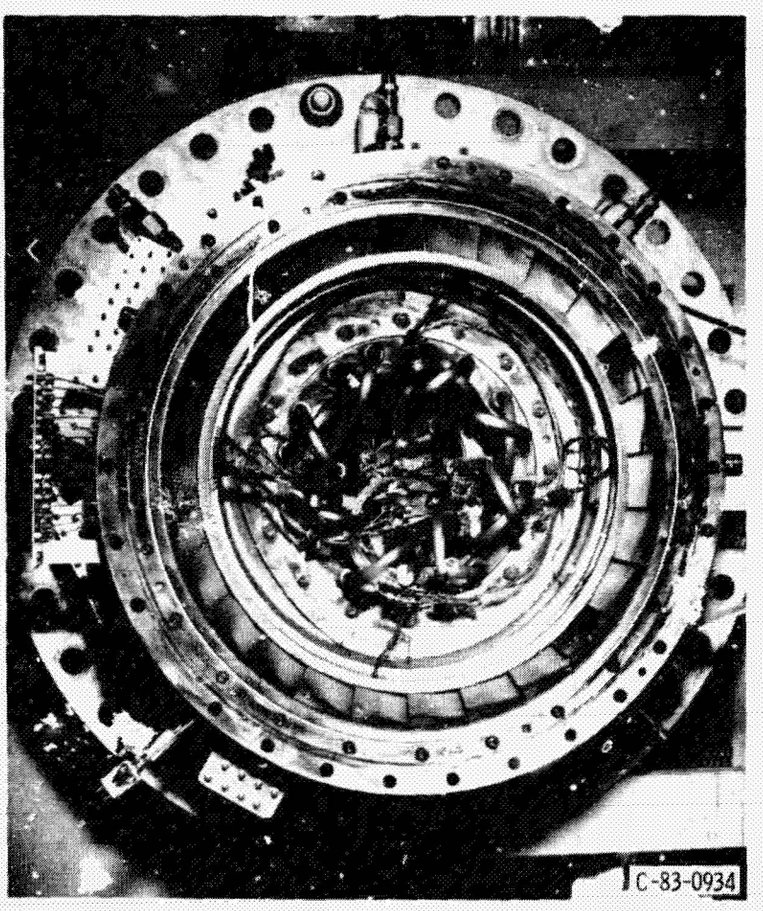

(a) Stator assembly.

Figure 3.

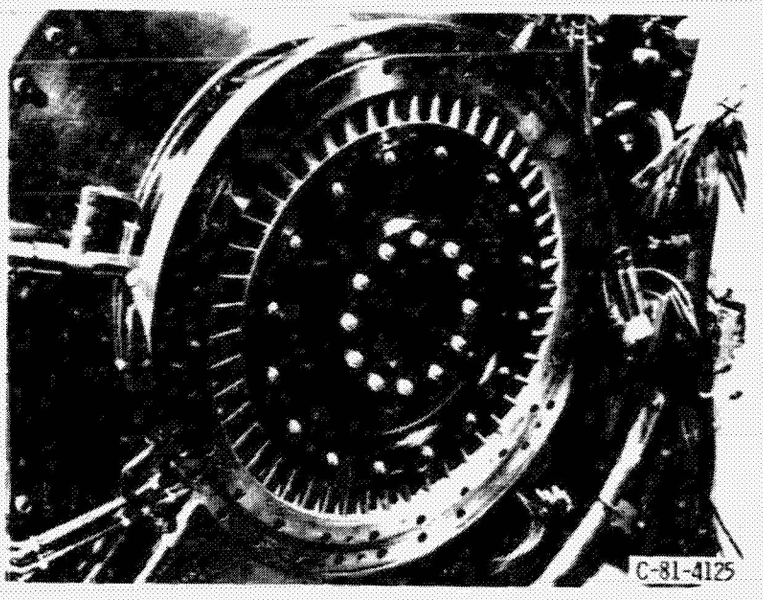

(b) Rotor installed in turbine test rig.

Figure 3. - Concluded.

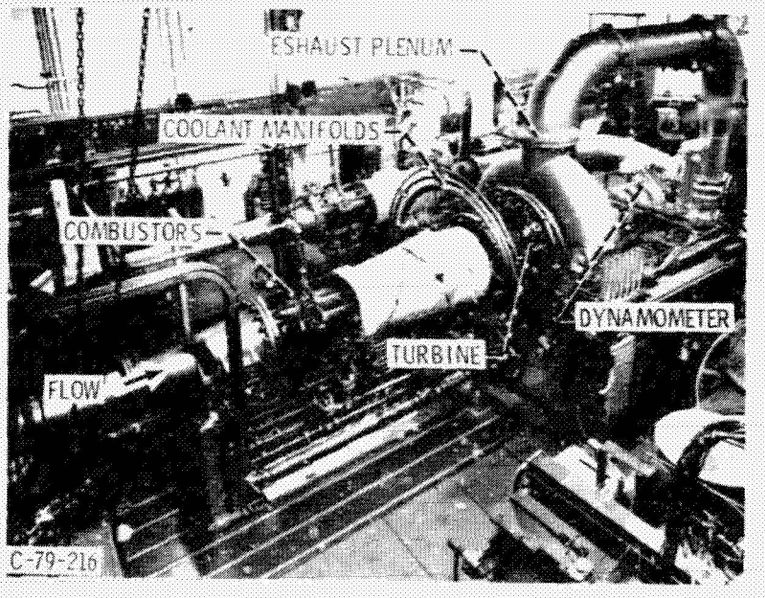

Figure 4. - Warm core turbine test facility.

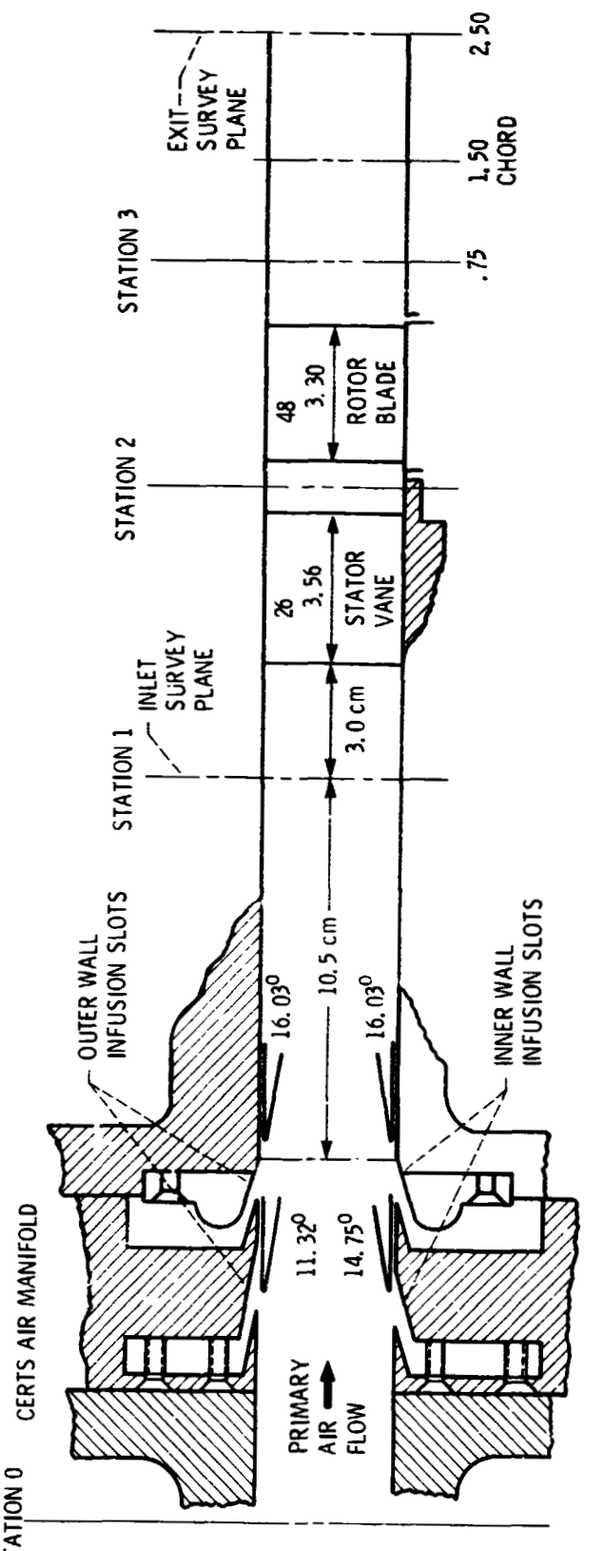

Figure 5. - Flowpath through turbine with CERTS inlet.

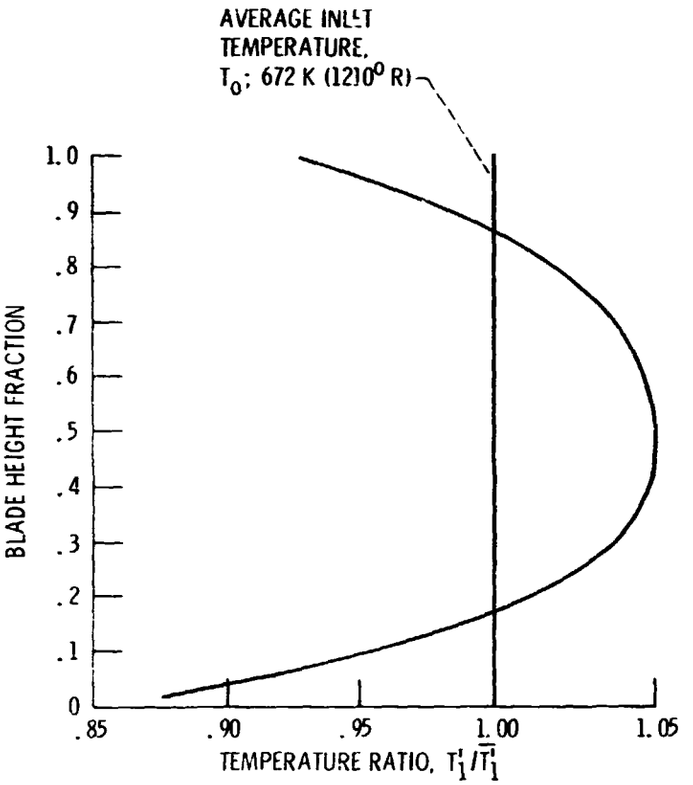

(a) Inlet radial temperature variation.

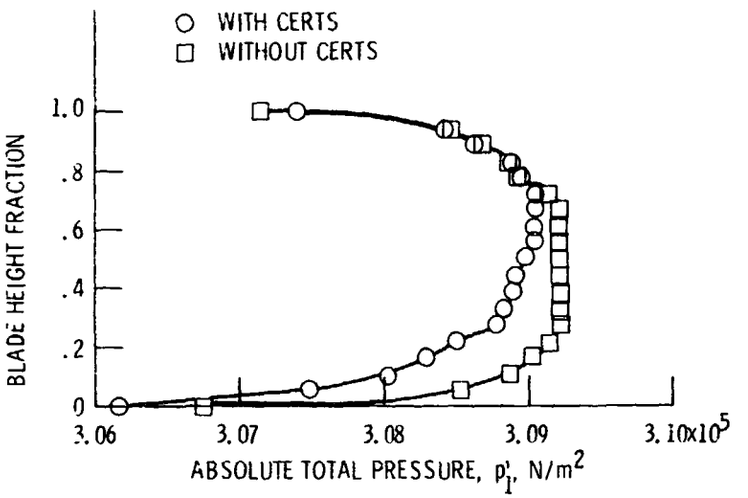

(b) Stator inlet pressure profiles.

Figure 6. - Turbine inlet conditions.

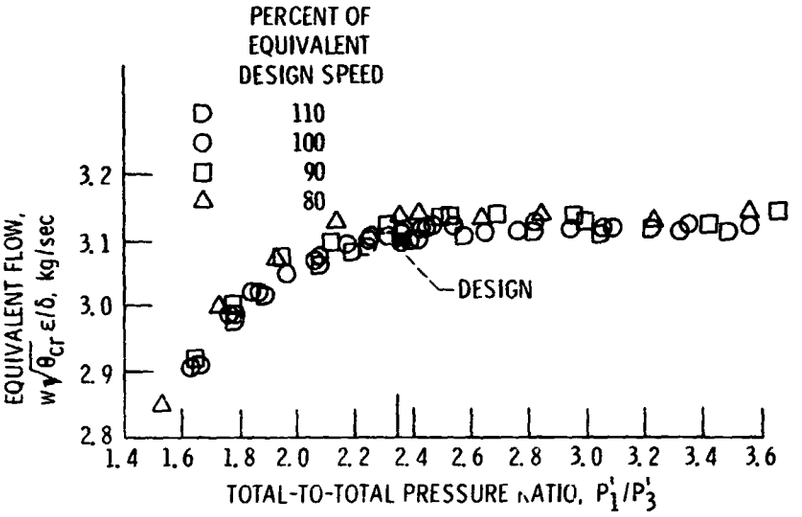

Figure 7. - Equivalent mass flow.

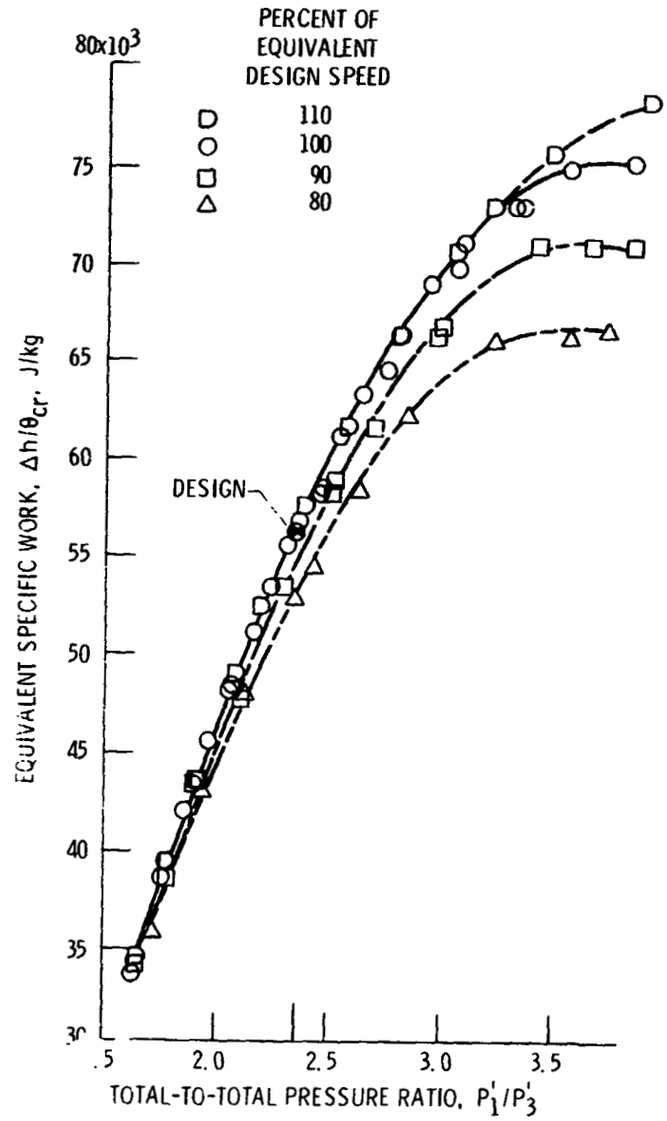

Figure 8. - Equivalent specific work.

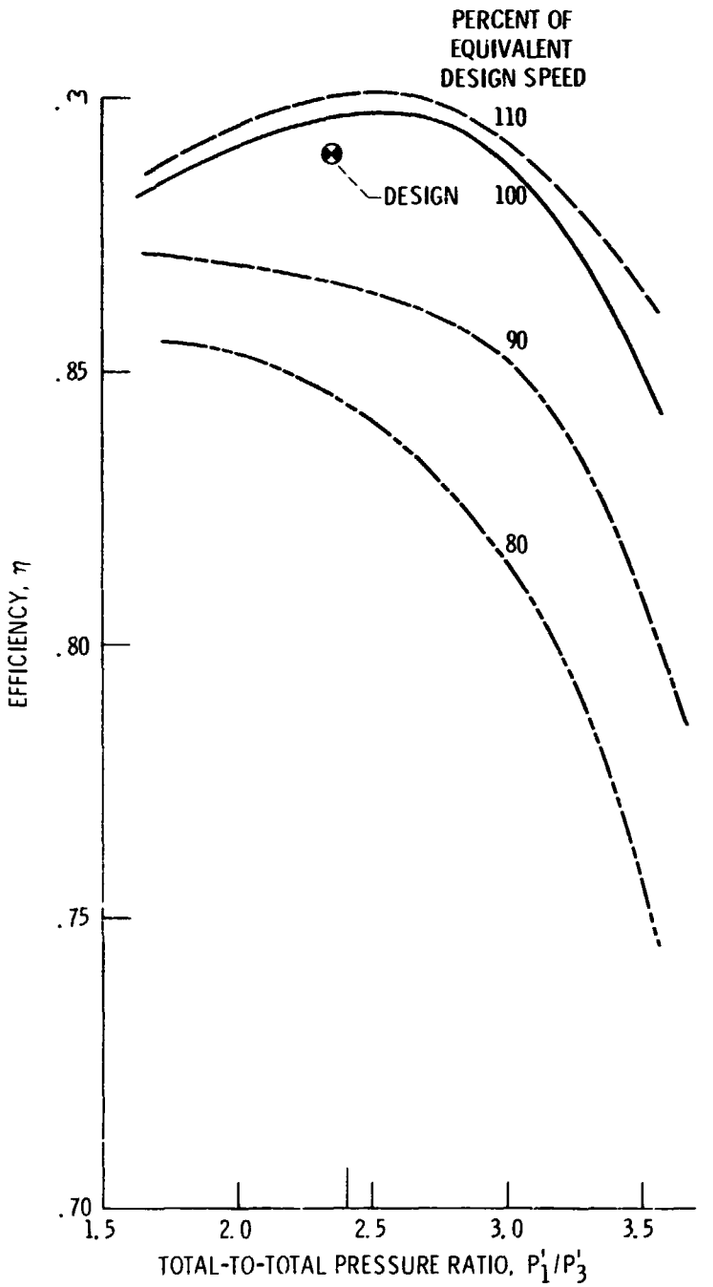

Figure 9. - Stage total efficiency.

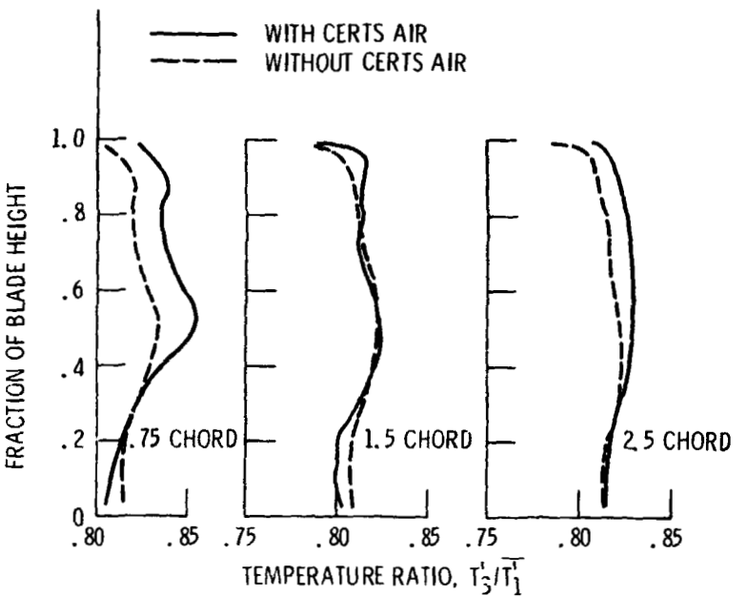

Figure 10. - Comparison of exit radial temperature variation with uniform inlet and inlet radial temperature profile.

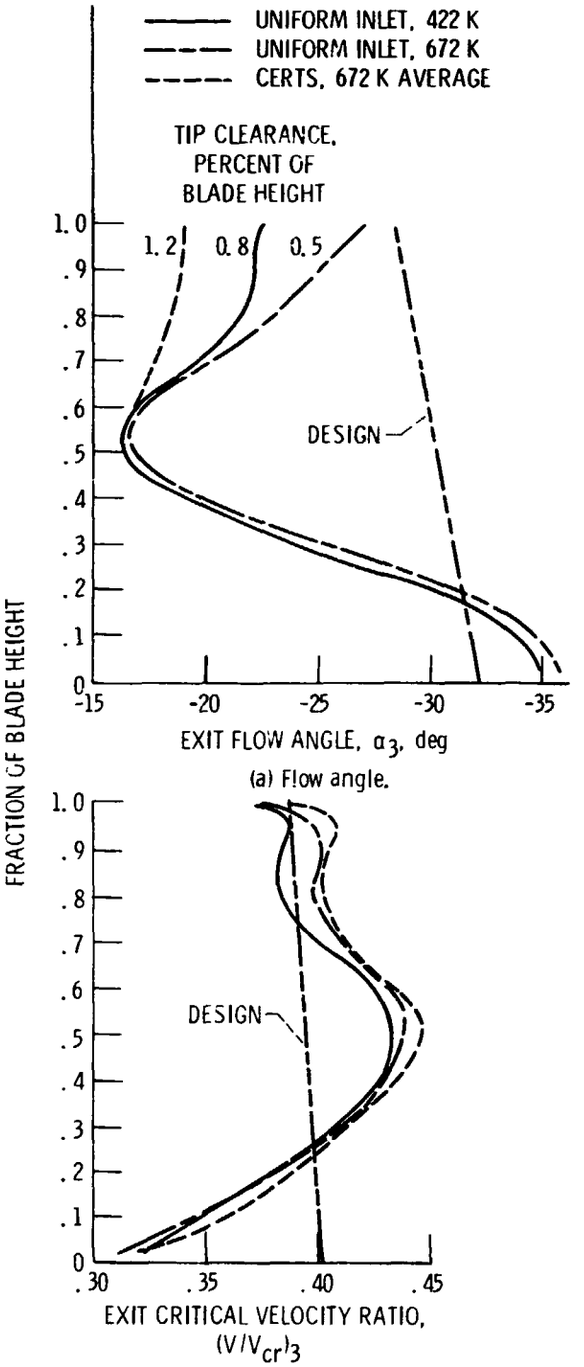

Figure 11. - Radial variation of rotor exit flow conditions, 2.5 chords axially downstream.

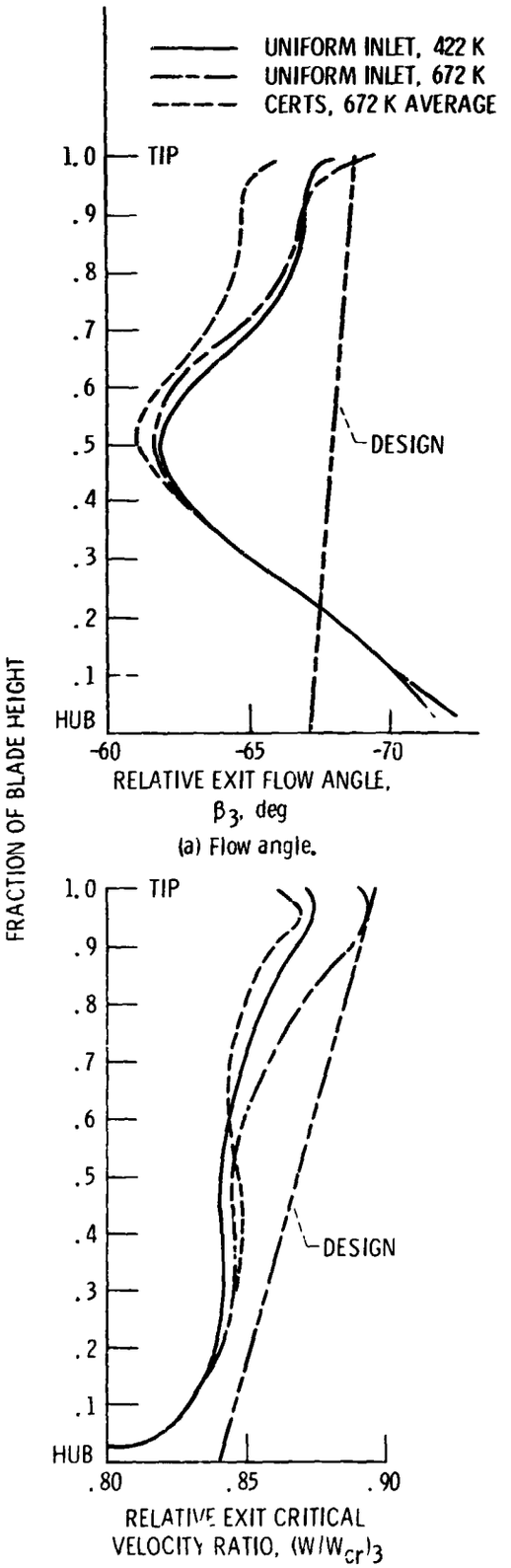

(a) Flow angle.

(b) Velocity ratio.

Figure 12. - Radial variation of rotor exit relative flow conditions, 2.5 chords axially down stream.

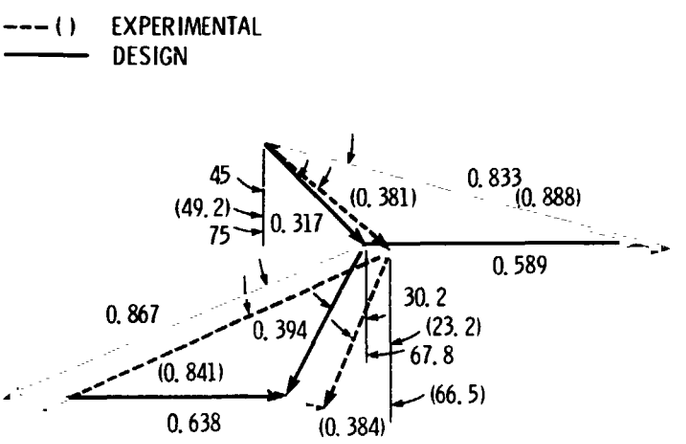

Figure 13. - Comparison of design and experimentally determined mean section velocity diagrams for uniform inlet conditions, 422 K.